

# RECOVERY OF RAT MUSCLE SIZE BUT NOT FUNCTION MORE THAN 1 YEAR AFTER A SINGLE BOTULINUM TOXIN INJECTION

SAMUEL R. WARD, PT, PhD,<sup>1,2,3</sup> VIVIANE B. MINAMOTO, PT, PhD,<sup>1</sup> KENTARO P. SUZUKI, MD,<sup>1</sup>  
JONAH B. HULST, MD,<sup>1</sup> SHANNON N. BREMNER,<sup>1</sup> and RICHARD L. LIEBER, PhD <sup>1,2,4</sup>

<sup>1</sup>Department of Orthopaedic Surgery, University of California San Diego, La Jolla, California, USA

<sup>2</sup>Department of Bioengineering, University of California, San Diego, La Jolla, California, USA

<sup>3</sup>Department of Radiology, University of California, San Diego, La Jolla, California, USA

<sup>4</sup>Rehabilitation Institute of Chicago, 345 East Superior Street, Chicago, Illinois 60611, USA

Accepted 23 May 2017

**ABSTRACT:** *Introduction:* Neurotoxin injection is used to treat a wide variety of neuromuscular disorders. The purpose of this study was to measure the functional and structural properties of botulinum toxin-injected adult rat skeletal muscle over nearly the entire lifespan. *Methods:* Ten groups of animals were subjected to either neurotoxin injection [Botox, Type A (BT-A); Allergan, Irvine, California] or saline solution injection. Neurotoxin-injected animals ( $n = 90$ ) were analyzed at different time-points: 1 week; 1 month; 3 months; 6 months; 12 months; or 18 months. *Results:* In spite of the recovery of structural features, such as muscle mass and fiber area, dorsiflexion torque production remained significantly depressed by 25%, even at 12 months after neurotoxin injection. *Discussion:* The data demonstrate that, after a single BT-A injection, although gross muscle morphology recovered over a 12-month time period, loss of contractile function did not recover.

*Muscle Nerve* 57: 435–441, 2018

Neurotoxin injection is commonly used to treat a variety of neuromuscular disorders. In light of the number and variety of neurotoxin injections, as well as the economic impact of this procedure, it is of great interest to optimize injection efficiency, minimize side effects, and understand the effects on muscle. Although rare,<sup>1,2</sup> the side effects of generalized weakness, excessive loss of muscle tone, neurotoxin spread to adjacent regions, and even death<sup>3</sup> highlight the need to establish best practices for neurotoxin injection and to fully understand the nature of botulinum neurotoxin type A (BT-A) effects on the target organ—skeletal muscle.

Additional supporting information may be found in the online version of this article.

**Abbreviations:** BT-A, onabotulinum toxin A neurotoxin; CSA, cross-sectional area; EDL, extensor digitorum longus; EHL, extensor hallucis longus; MHC, myosin heavy chain; NMJ, neuromuscular junction; SDS-PAGE, sodium dodecylsulfate–polyacrylamide gel electrophoresis; TA, tibialis anterior

**Key words:** aging; Botox; denervation neurotoxin; muscle fiber type; muscle physiology; neuromuscular junction

**Funding:** Department of Veterans Affairs (RX000670); National Institutes of Health (grants R24HD050837 and AR057013); and Allergan, Inc.

**Conflicts of Interest:** R.L.L. was a paid consultant to Allergan, Inc., during the course of this study. He also receives textbook royalties from Wolters Kluwer.

**Correspondence to:** R.L. Lieber; e-mail: rlieber@ric.org

© 2017 Wiley Periodicals, Inc.  
Published online 26 May 2017 in Wiley Online Library (wileyonlinelibrary.com).  
DOI 10.1002/mus.25707

Because neurotoxin injection affects muscle mechanical function as well as its innervation, it is important to measure multiple structural and functional muscle properties when attempting to assess the effects of BT-A administration. For example, loss of voluntary or electrically induced muscle force could occur from decreased muscle fiber size, decreased number of innervated fibers, or a combination of the two. In extreme cases, alterations in myosin heavy chain (MHC), the major muscle contractile protein, could also cause force alteration.<sup>4,5</sup> To date, most studies have measured only a few of these properties and assumed a functional correlate (if structure was measured) or a structural correlate (if function was measured). In addition, because the effects of BT-A can be systemic,<sup>6</sup> it is important to differentiate the direct effects of toxin injection from those occurring systemically. Because we are also interested in the long-term effects of BT-A, a control group receiving only saline injection must also be employed to differentiate muscle performance changes due to BT-A injection from those that occur naturally with aging.

To address these concerns, we developed a highly accurate animal model in which the contractile properties of the rat dorsiflexor muscles can be measured with a coefficient of variation of only 10%,<sup>7</sup> and we analyzed dorsiflexion torque and structural and biochemical properties of these muscles after a single toxin injection.<sup>6</sup> Given this low variability, effect sizes of ~10% can easily be detected. We used this model to study the relationship between injection dose and volume<sup>8</sup> on function, the effects of joint manipulation on efficacy and side effects,<sup>6</sup> the effect of multiple injections,<sup>9</sup> and even defined the complete transcriptional profile of muscle at various time-points after injection.<sup>10,11</sup> These earlier studies pointed to an asynchronous response by muscle cells in which silencing of the neuromuscular junction (NMJ) secondary to cleavage of the synaptosomal-associated protein-25 protein led to rapid and transient transcriptional changes, but persistent functional changes. However, like others, our earlier studies were performed at a single time-point or used

primarily a single method. To fully characterize muscle's response to BT-A, multiple measurements must be made over a reasonable time span at reasonable intervals. Therefore, the purpose of this study was to measure the functional properties of normal adult rat skeletal muscle over most of the rat's lifespan (18 months, which is about three fourths of the rat lifespan)<sup>12</sup> while also quantifying muscle fiber size, fiber type, collagen content, and titin in an attempt to understand the structural correlates to the functional changes observed. Our aim was to define the natural history of muscle's response to BT-A injection and to understand the underlying basis for changes in muscle function after a single, therapeutic dose of BT-A.

## METHODS

**Animal Subjects.** Animals used in this study included 90 untrained, mature, male Sprague-Dawley rats (Harlan, Indianapolis, Indiana) with an average weight of  $399 \pm 29$  g (mean  $\pm$  SD). Rats were housed 2 per cage at 20°–23°C with a 12h:12h dark:light cycle. All procedures were approved by the committees on the use of animal subjects in research at the University of California and the VA Medical Center. After terminal physiological experiments, animals were euthanized with an intracardiac injection of pentobarbital sodium (0.5 ml of 390-mg/ml solution).

**Experimental Model.** Animals were randomly divided into 10 groups, and subjected to either BT-A injection (Botox, Type A; Allergan, Irvine, California) or saline solution injection. Neurotoxin-injected animals were analyzed at different time-points: 1 week ( $n = 8$ ); 1 month ( $n = 19$ ); 3 months ( $n = 8$ ); 6 months ( $n = 8$ ); 12 months ( $n = 9$ ); or 18 months ( $n = 6$ ). Five groups of saline-injected animals, at 1 week ( $n = 4$ ), 1 month ( $n = 4$ ), 3 months ( $n = 4$ ), 6 months ( $n = 4$ ), 12 months ( $n = 10$ ), or 18 months ( $n = 6$ ), served as controls for anesthesia, handling, aging, and injection procedures. The investigators were not blinded to the experimental intervention or the identities of the experimental groups.

After anesthesia induction (2% isoflurane, 2.0 L/min), ankle isometric dorsiflexion torque was measured before injection, as described elsewhere.<sup>7</sup> Briefly, dorsiflexors were activated via the common fibular nerve, whereas torque was measured using a custom-designed dynamometer.<sup>7</sup> The dynamometer was created from a dual-mode servo motor (Model 305B; Aurora Scientific, Aurora, Ontario, Canada), which has a force resolution of 1 mN, a linearity of 99.8%, and a step response time of <2 ms. The fibular nerve innervates the anterior compartment as well as the peroneus muscles. The peroneus longus and brevis produce a slight plantarflexion torque, whereas the anterior compartment muscle [tibialis anterior (TA), extensor digitorum longus (EDL), and extensor hallucis longus (EHL)] produce a strong dorsiflexion torque. Based on the muscle architecture of the TA compared with the EHL and EDL,<sup>13</sup> the dorsiflexion torque produced is dominated by TA, which produces ~85% of the torque.<sup>7</sup>

Three contractions were averaged to yield the value for maximal isometric torque, which has been shown to have a coefficient of variation of about 10%,<sup>7,14</sup> enabling reliable resolution of small changes in dorsiflexor function. After determination of initial torque, rats received either a 1-time BT-A injection (dose 6.0 units/kg in a volume of 100  $\mu$ l) or

a 100- $\mu$ l volume of 0.9% NaCl solution into the midbelly of the TA muscle. This region was localized by palpating the largest bulk of the muscle, and the volume was administered by the same physician into 2 sites of the midbelly, as described elsewhere.<sup>8</sup>

At different time-points (1 week, and 1, 3, 6, 12, and 18 months), dorsiflexion torque was measured from both saline- and BT-A-injected groups in both hindlimbs to measure systemic and aging effects.

**Muscle Fiber Size Analysis.** Excised TA muscles were snap frozen in isopentane cooled by liquid nitrogen ( $-159^\circ\text{C}$ ) and stored at  $-80^\circ\text{C}$  for subsequent analysis. Muscle cross-sections (10  $\mu$ m thickness) were taken from the TA muscle midbelly. Sections were first treated with 1% bovine serum albumin and with normal goat and rat serum as blocking agents. Sections were incubated overnight with a polyclonal anti-laminin antibody (Sigma, St. Louis, Missouri; dilution 1:1,000), and then with the secondary antibody, goat anti-rabbit IgG (Alexa Fluor 594; Invitrogen, Carlsbad, California; dilution 1:200). The laminin antibody is used to label the fiber perimeter and facilitate fiber area quantification, as described elsewhere.<sup>6</sup>

Sections were imaged with a digital camera (Spot RT; Diagnostic Instruments, Sterling Heights, Michigan) on an epifluorescence microscope (Nikon Microphot SA; Nikon, Tokyo, Japan) using a 10 $\times$  objective with a G-2B filter set for red fluorescence.<sup>15</sup> Muscle fiber size and filtering criteria were applied to ensure measurement of actual muscle fibers and not connective tissue pieces or artifacts, as described elsewhere.<sup>6</sup> Regions with circularity below 0.30 or above 1.0 were excluded to prevent inclusion of fibers that were obliquely sectioned, which has the effect of artifactually increasing fiber area.<sup>16</sup>

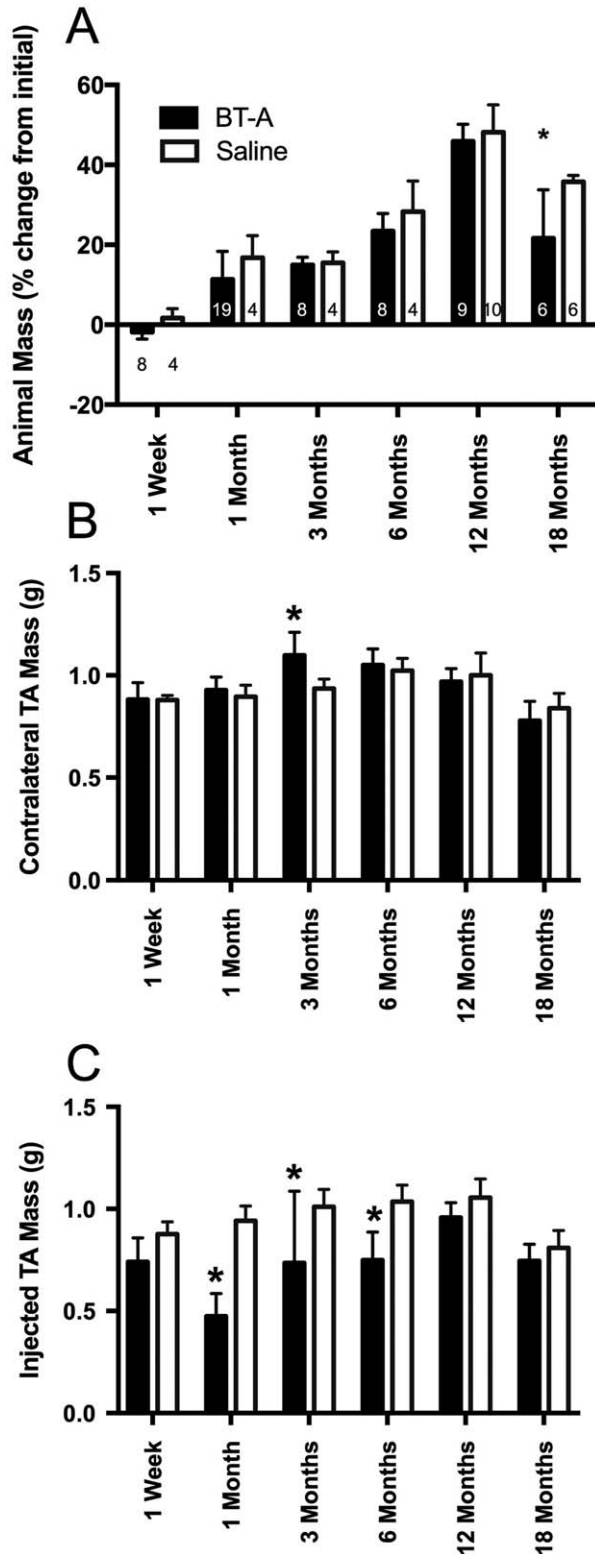
**Myosin Heavy Chain Analysis.** Myosin heavy chain (MHC) isoform distributions were determined by adapting a gel electrophoresis technique, as described elsewhere.<sup>17</sup> Muscles were homogenized, and the myofibril-rich pellets were washed and resuspended in buffers supplemented with a protease inhibitor cocktail (100  $\mu$ mol/L phenylmethylsulfonyl fluoride, 10  $\mu$ g/ml leupeptin, and 10  $\mu$ g/ml pepstatin A). Protein was then diluted in sample buffer to a concentration of 0.125 mg/ml across all muscle homogenates. Separation of MHC isoforms was performed with sodium dodecylsulfate-polyacrylamide gel electrophoresis (SDS-PAGE; 16 cm  $\times$  22 cm, thickness 0.75 mm) with 22 h of migration at 275 V at 4°C. Stacking and resolving gels were 4% and 8% polyacrylamide, respectively. Gels were silver stained according to the manufacturer's instructions (Bio-Rad, Hercules, California). The positions of MHC isoforms were determined by their relative electrophoretic mobilities, which have been characterized extensively in previous work.<sup>17–19</sup>

**Statistical Analysis.** Experimental results were analyzed by 2-way analysis of variance with repeated measures using treatment group and testing time as grouping factors. *Post-hoc* Sidak tests were used to compare dependent variables among various pairs of groups. Relationships between muscle fiber area and torque were quantified by linear regression. All results are reported as mean  $\pm$  SEM unless otherwise noted.

**Previous Publication of Data Subset.** Three subsets of these data were reported as part of 3 previous studies.<sup>7,9,11</sup> Details of the specific data sets are provided in the Supplementary Material available online.

## RESULTS

Animals from both the BT-A and saline groups had increased body mass through 12 months, which then declined from 12 to 18 months due to the normal developmental and aging process (Fig. 1A). Body mass increased by about 50% throughout this study. Although the only statistically significant



difference in body mass between groups was observed at 18 months, animals in the BT-A group lost about 3% of their body mass, on average, over the first week. Contralateral TA muscle mass remained relatively constant between 3 and 12 months, and declined between 12 and 18 months (Fig. 1B). In contrast, muscles injected with BT-A showed a significant decline in muscle mass after 1 month, began to recover at 3 and 6 months, but remained lower than in the contralateral side until about 12 months (Fig. 1C). Because the mass of the TA is only about 1 g, changes in animal mass did not simply result from changes in TA mass.

Qualitatively, the morphology of BT-A-injected TA muscles at different time-points was as expected. In control muscles and muscles before injection, we observed tightly packed polygonal fibers with peripheral myonuclei and minimal mononuclear cells in the extracellular space. One week after injection, morphology was still fairly normal (Fig. 2A), but, after 1 month, the obvious change observed was decreased muscle fiber size with increased heterogeneity, as previously reported<sup>8</sup> (Fig. 2B), which persisted at the 3-month time-point (Fig. 2C). By 6 months, the tissue showed some regions of near normal fiber size and some regions of decreased fiber size, which were slightly hypercellular. Central nuclei were occasionally observed, indicating some degree of fiber regeneration (Fig. 2D). Morphology of muscles at both 12 and 18 months (Fig. 2E and F) was indistinguishable from that of saline-injected muscles (not shown). Muscle fiber cross-sectional area (CSA) correlated with muscle mass ( $r^2 = 0.67$ ,  $P < 0.0001$ ), suggesting that a major fraction of the change in muscle mass was due to muscle fiber atrophy. Quantification of fiber area revealed that the largest decrease in fiber CSA was observed 1 month after injection, at which point it was only 28% of the value measured after saline injection (Fig. 3A). Fiber

**FIGURE 1.** (A) Body mass of animals injected with BT-A (filled bars) or saline (open bars) relative to the initial body mass. Note that mass increases and then decreases due to normal developmental and then aging processes. Data represent mean  $\pm$  SEM of 90 animal subjects (4–19 per group; sample size shown on bar). Asterisk indicates significant difference between saline-injected and BT-A-injected groups at a given time-point ( $P < 0.05$ ). Mass of TA muscles (B) contralateral to muscles injected with BT-A (filled bars) or saline (open bars) and (C) muscles injected with BT-A (filled bars) or saline (open bars). Note that no difference was observed between BT-A and saline (open bars) for contralateral control muscles, except for a spurious value at 3 months, indicating lack of a systemic effect. However, significant effects of BT-A were observed at early time-points. Data represent mean  $\pm$  SEM (4–19 per group). Asterisk indicates significant difference between the saline-injected and BT-A-injected groups at a given time-point ( $P < 0.05$ ).

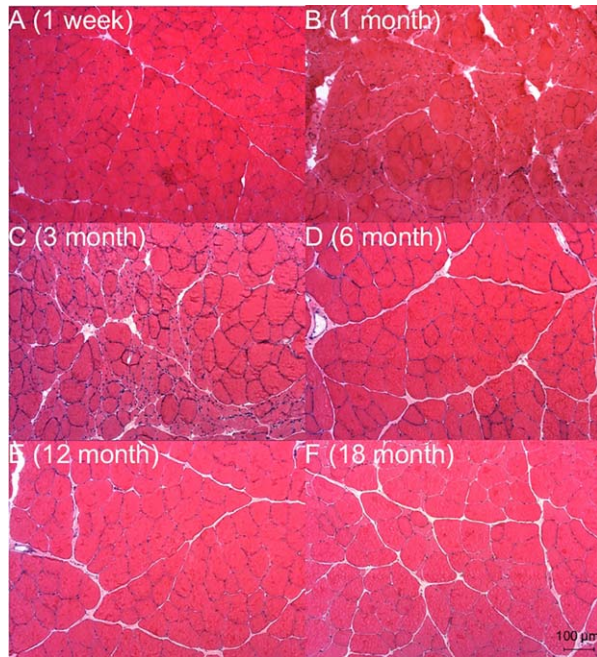


**FIGURE 2.** Representative histological sections of TA muscles at 1 week (A), 1 month (B), 3 months (C), 6 months (D), 12 months (E), and 18 months (F) after BT-A injection compared with saline-injected control (G). Fiber size heterogeneity and increased cellularity was observed at 1 month (B) and 3 months (C). At these time-points, some fibers still retain normal size and morphology, even though they are surrounded by highly atrophic fibers. Bar = 100  $\mu\text{m}$ .

CSA gradually recovered to 63%, 74%, and 96% of contralateral values at 3, 6, and 12 months, respectively, and showed no difference compared with the saline injection group at either 12 or 18 months ( $P > 0.4$ ; Fig 3A). Fiber area on the contralateral muscles showed the same change as a function of age that was observed for muscle mass (Fig. 1B); that is, a gradual increase until about 12 months of age, followed by a mild decline at 18 months of age.

Although muscle mass and fiber size recovered after 12–18 months to levels observed in saline-injected animals and contralateral controls, dorsiflexion torque production was significantly decreased at all time-points from 1 week to 12 months when compared with saline control groups (Fig. 4A). Negative dorsiflexion torque was observed at 1 week, presumably due to activation of peroneal muscles. Dorsiflexion torque gradually recovered to 45% and 50% of saline values at 3 and 6 months, respectively, and, after 1 year, BT-A-injected muscles generated  $\sim 73\%$  of the torque generated by saline-injected muscles (Fig. 4A). The greatest variability in torque was observed for the 3-month experimental group, presumably due to variations in the rate of recovery from BT-A injection. Between 12 and 18 months of age, all groups decreased in torque generation, presumably due to age-related changes based on the fact that the decrease was observed in both the injected

and contralateral limbs from the saline group (Fig. 4B). At the 18-month time-point, BT-A-injected and saline-injected muscles generated the same torque (Fig. 4A).

Several other biochemical assays revealed a minor response to BT-A injection. There was generally no change in titin mass as a function of time or between BT-A-injected and saline-injected muscles (refer to Table S1 in the Supplementary Material available online), with the single exception being a very small increase in titin mass for the BT-A-injected muscles and their contralateral muscles at 1 month. Collagen content in the TA muscles was variable and somewhat irregular (see

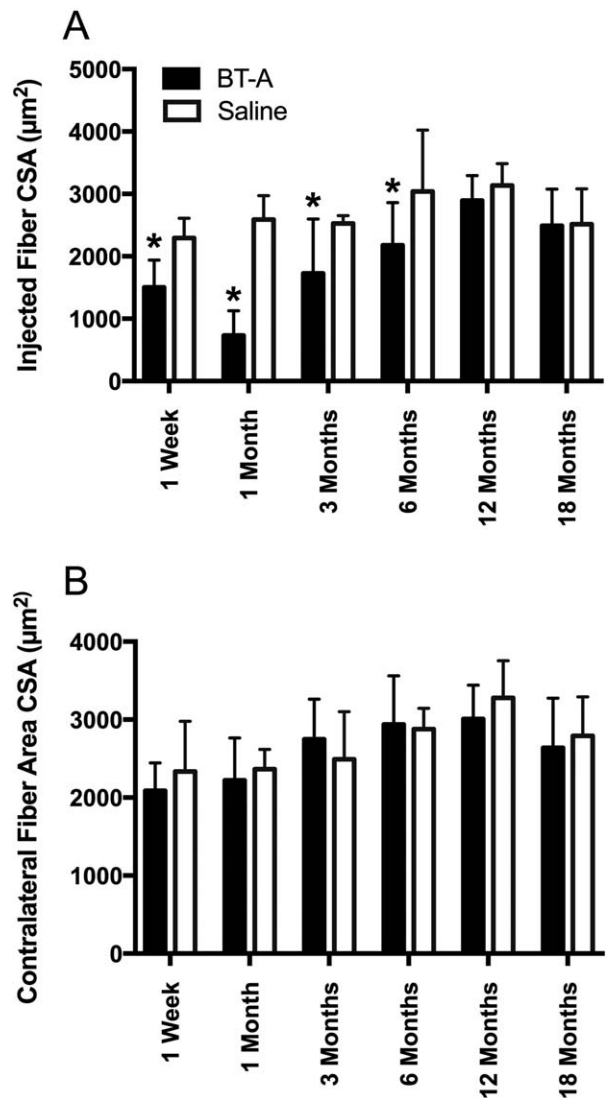


**FIGURE 3.** Muscle fiber cross-sectional areas of TA muscles (A) injected with BT-A (filled bars) or saline (open bars) and contralateral muscles (B). Note that muscle fiber area recovered in the BT-A group by 12 months of age. This is in contrast to functional results (cf. Fig. 5). Data represent mean  $\pm$  SEM (4–12 per group). Asterisk indicates significant difference between saline-injected and BT-A-injected groups at a given time-point ( $P < 0.05$ ).

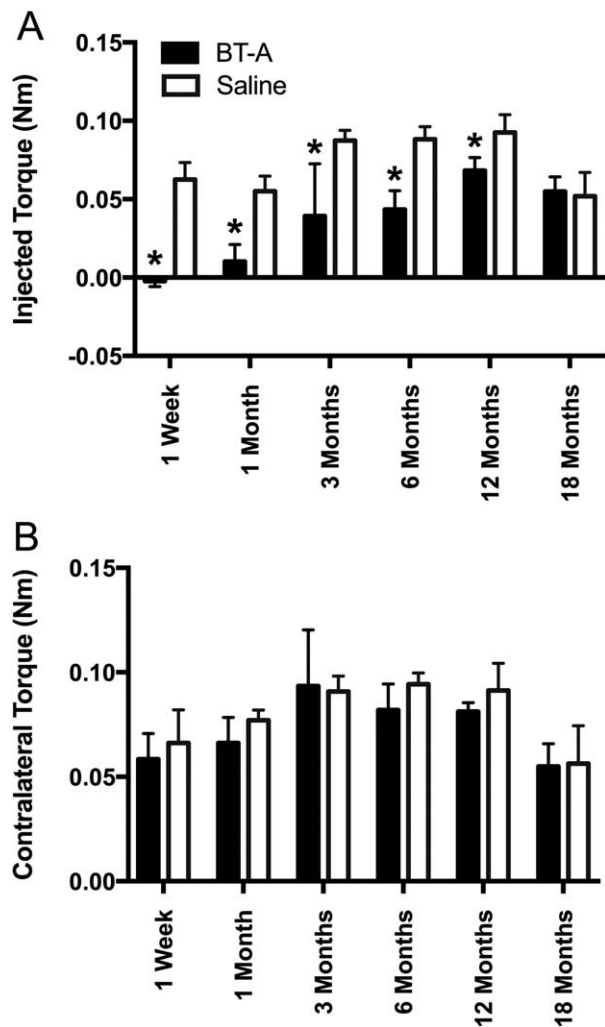


**FIGURE 4.** Dorsiflexion torque measured from animal subjects (A) injected with BT-A (filled bars) or saline (open bars) and (B) contralateral muscles. Note the negative torque 1 week after BT-A injection and, although a gradual recovery can be seen, torque was still lower than saline-injected muscles after 12 months. Data represent mean  $\pm$  SEM (4–19 per group). Asterisk indicates significant difference between saline-injected and BT-A-injected groups at a given time-point ( $P < 0.05$ ).

Table S2 online). Overall, collagen content increased in the BT-A-injected muscles at the earlier time-points. With regard to the contractile protein, MHC, high levels of type IIB MHC were expressed, followed by types IIX, IIA, and I (see Table S3 online). After BT-A injection, there was a significant increase in the expression of type I isoform at the expense of the fastest isoform (type IIB). Higher expression of type I muscle fiber was observed 1, 3, 6, and 18 months after BT-A injection when compared with saline injection ( $P < 0.05$ ; see Table 3 online). However, although statistically significant, the magnitude of this effect was extremely small, with type I MHC increasing from  $\sim 4\%$  to  $\sim 7\%$  of the total MHC pool.

Dorsiflexion torque correlated with TA fiber area as a function of time and treatment (Fig. 5, and Table S4 online). After 1 and 3 months there was a significant relationship ( $r^2 > 0.6$ ) between the 2 parameters, suggesting that the functional recovery was due to muscle fiber size recovery. After 6 months, there was no longer a correlation between the 2 parameters, demonstrating that something other than muscle fiber size was responsible for the functional variability of these BT-A-injected muscles.

## DISCUSSION

The results of this study reveal an asynchronous change in muscle fiber size, which did not track dorsiflexor functional properties completely. We observed a persistent loss in muscle contractile function even 1 year after a single BT-A injection, a time-point at which all of the measured structural and biochemical parameters had returned to normal levels. Therefore, these data indicate that, after a single BT-A injection, although gross muscle morphology recovers over a 12-month time period, loss of contractile function persists.<sup>20</sup>

The most rapid change observed was loss of dorsiflexion torque, presumably due to blockade of the NMJ, the mechanism of BT-A action.<sup>21</sup> This blockage sets off a complex muscle transcriptional response involving  $\sim 2,000$  genes<sup>11</sup> that leads to relatively rapid loss in muscle fiber size and mass over the first month.<sup>6</sup> This loss in muscle mass is due to upregulation of genes involved in destabilization of the NMJ (*Chrna1*, *Chrne*) as well as muscle genes involved in catabolic processes or atrophy (*Nfkb*, *Tgf- $\beta$* , *Fbxo32*). The net result of this transcriptional activity is rapid loss of muscle mass and, thus, at this 1-month period, from a transcriptional point of view, the effect of BT-A has essentially been completed. Based on our previous study,<sup>11</sup> there

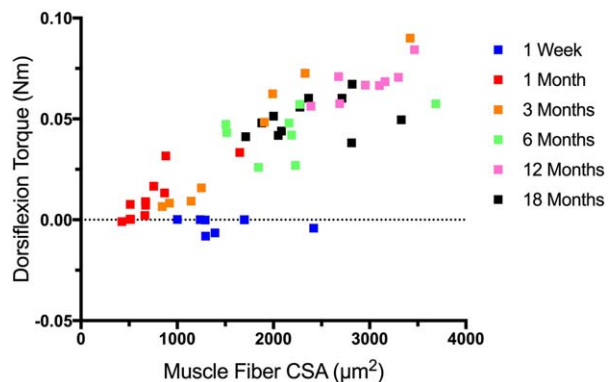


**FIGURE 5.** Relationship between muscle fiber cross-sectional area (CSA) and dorsiflexion torque for the BT-A-injected muscles. Each symbol represents a different time period. Regression coefficients and statistical analysis for each group are presented in Table S4 (refer to Supplementary Material online).

are only 32 transcripts that are expressed over control levels after the first month and these primarily relate to rebuilding lost muscle mass (*Myhl2*, *Myhl3*, *Tmod1*, *Ryr1*). These experiments indicate that NMJ blockade sets off a very rapid biological response that requires nearly the rest of the rat's lifetime to recover fully.

Because muscle structural and functional properties were measured from the same animal subjects, it was possible to apply correlation analysis to these structure-function data to gain insight into the relationship between the two. As expected, there was no significant correlation between fiber area and torque after 1 week. This is because the NMJ had been paralyzed rendering the muscle inactive, but the fibers had not yet had sufficient time to atrophy. This resulting asynchrony between biology, structure, and function is most clearly seen by comparing muscle fiber area (structure) to dorsiflexion torque (function) across the time-points measured. At the earliest time period measured after injection (1 week), torque decreased dramatically (Fig. 4A), even though muscle fiber area had not changed, presumably because the NMJ had been blocked (Fig. 3A). Then, muscle fiber size began to decrease in response to chemodenervation and torque remained low (1 month; see Figs. 2B and 3A). Subsequently, during intermediate time periods (3–6 months; see Figs. 2C and D and 3A), both muscle fiber area and dorsiflexion torque recovered, albeit at different rates. Muscle fiber area recovered with an approximately 6-month half-life and was essentially at control levels 1 year after injection and indistinguishable from control muscle. Interestingly, torque was only about 75% of control values at this time-point (Fig. 4A). Because muscle fiber size was near normal, and the MHC isoform distribution was not dramatically altered (see Table S2 online), our interpretation of these results is that the muscle fibers were not normally functional, even 1 year after BT-A injection. The mechanistic site for this dysfunction could be the NMJ or the muscle fiber itself. From these data, we cannot distinguish between the two. However, if fibers are normally sized, but function remains depressed, this indicates that, after a single BT-A injection, the initial chemodenervation sets off a rapid transcriptional response lasting weeks, muscle fiber size changes lasting many months, and neuromuscular reorganization that can require nearly the entire rat lifetime for full recovery. Evidence for such irreversible denervation and reinnervation was provided in a recent study quantifying fiber type grouping after BT-A injection.<sup>9</sup> The mechanistic detail for such a response is not yet settled—whether the muscle fibers had the correct number and distribution of

NMJs that simply did not function normally or whether the normal NMJ did not form. It has been stated that, after application of BT-A, the NMJ reforms in its original location with normal structure.<sup>22</sup> However, physiological function of these NMJs with regard to quantal acetylcholine release, calcium currents, and other subcellular events has not been definitively tested.<sup>23</sup> The fact that contralateral and saline-injected muscles showed similar structure and function suggests that the BT-A injection acted locally on the TA muscle, did not cause a significant systemic complication, and that normal rat development occurred in spite of the BT-A injection (Fig. 3B).

Analysis of the extracellular environment revealed a major increase in collagen concentration (see Table S2 online). Although this was reported in a previous study,<sup>8</sup> our interpretation of this measured collagen increase is that it actually overrepresents the collagen response due to the selective loss of muscle fiber area (Fig. 3) and the fact that collagen is expressed per unit muscle mass. Because there is no quantitative model for the relationship between muscle fibers and extracellular collagen,<sup>24</sup> it is not possible to convert collagen concentrations (micrograms of collagen per milligram tissue) into absolute numbers of collagen molecules per fiber. Based on the muted transcriptional response of extracellular matrix molecules<sup>11</sup> and the relatively large muscle fiber area change, we cannot conclude that BT-A application induces a strong extracellular fibrotic response.<sup>25</sup> The increase in collagen may also be confounded with the aging response. Indeed, it has been reported that aging results in increased slow MHC expression, and the saline group did show a slight reduction in type IIB and an increase in type IIX beginning at 6 months (see Table S3 online). Regarding titin, we confirmed the minor changes previously reported for the giant intramuscular protein,<sup>27</sup> which accompanied changes in the elastic modulus of muscle cells.<sup>27</sup>

Because the current study was performed on normal muscle throughout the lifetime of the rat, the findings are not immediately applicable to the clinical use of BT-A on human spastic muscle contractures. This is because spastic muscle is already highly deranged with regard to its transcriptional profile,<sup>28</sup> biomechanical properties,<sup>29–31</sup> and sarcomere length.<sup>32,33</sup> It is thus unknown whether the upper motor neuron lesion effects would be minimized or enhanced by blocking the NMJ. However, there are no animal models that recapitulate human spasticity. Importantly, the current data do not provide support for the generally accepted practice of treating spasticity in humans with BT-A injections every 3–6 months.<sup>34</sup> After 3–6 months in

our model system, muscle fiber size recovered to ~70% of normal and function to ~50% of normal. Based on the entirety of this study, we suggest that this altered function was due to inappropriate muscle innervation combined with moderate muscle atrophy in the time frame considered reasonable for clinical redosing. This is because even only 50% of normal muscle function may be sufficient to create a joint contracture requiring further neurotoxin treatment.

Another reason that these data may not apply to human studies is that the injectate volume (100  $\mu$ l) is large relative to the size of the rat anterior compartment (1 ml<sup>8</sup>, but the dose (6.0 units/kg) is similar to that given to children. Much smaller relative volumes can be injected into large human muscles, and it is possible that these smaller volumes would produce results different than those observed in the current study.

In conclusion, in this study we have demonstrated that muscles respond to a single BT-A injection with a rapid transcriptional response followed by a relatively long period of neuromuscular remodeling. Although muscle fiber size and mass recover after 1 year, functional properties do not fully recover in that time frame. The precise mechanism for the functional loss is unknown, but may be related to hampered NMJ function or impaired muscle fiber excitation-contraction coupling. Future studies will be required to fully understand the mechanism of BT-A action. Such an understanding may improve our understanding of neuromuscular function and provide insights into the optimal clinical application of BT-A in medicine.

## REFERENCES

- Papavasiliou AS, Nikaina I, Foska K, Bouros P, Mitsou G, Filiopoulos C. Safety of botulinum toxin A in children and adolescents with cerebral palsy in a pragmatic setting. *Toxins* 2013;5:524-536.
- Mancini F, Sandrini G, Moglia A, Nappi G, Pacchetti C. A randomized, double-blind, dose-ranging study to evaluate efficacy and safety of three doses of botulinum toxin type A (Botox) for the treatment of spastic foot. *Neuro Sci* 2005;26:26-31.
- Li M, Goldberger BA, Hopkins C. Fatal case of BOTOX-related anaphylaxis? *J Forens Sci* 2005;50:169-172.
- Lieber RL, Johansson CB, Vahlsing HL, Hargens AR, Feringa ER. Long-term effects of spinal cord transection on fast and slow rat skeletal muscle. I. Contractile properties. *Exp Neurol* 1986;91:423-434.
- Lieber RL, Fridén JO, Hargens AR, Feringa ER. Long-term effects of spinal cord transection of fast and slow rat skeletal muscle. II. Morphometric properties. *Exp Neurol* 1986;91:435-448.
- Minamoto VB, Hulst JB, Lim M, Peace WJ, Bremner SN, Ward SR, *et al.* Increased efficacy and decreased systemic-effects of botulinum toxin A injection after active or passive muscle manipulation. *Dev Med Child Neurol* 2007;49:907-914.
- Peters D, Barash IA, Burdi M, Yuan PS, Mathew L, Fridén J, *et al.* Asynchronous functional, cellular and transcriptional changes after a bout of eccentric exercise in the rat. *J Physiol (Lond)* 2003;553:947-957.
- Hulst JB, Minamoto VB, Lim MB, Bremner SN, Ward SR, Lieber RL. Systematic test of neurotoxin dose and volume on muscle function in a rat model. *Muscle Nerve* 2014;49:709-715.
- Minamoto VB, Suzuki KP, Bremner SN, Lieber RL, Ward SR. Dramatic changes in muscle contractile and structural properties after 2 botulinum toxin injections. *Muscle Nerve* 2015;52:649-657.
- Smith LR, Meyer G, Lieber RL. Systems analysis of biological networks in skeletal muscle function. *Wiley Interdiscip Rev Syst Biol Med* 2013;5:55-71.
- Mukund K, Mathewson M, Minamoto V, Ward SR, Subramaniam S, Lieber RL. Systems analysis of transcriptional data provides insights into muscle's biological response to botulinum toxin. *Muscle Nerve* 2014;50:744-758.
- Sengupta P. The laboratory rat: relating its age with human's. *Int J Prevent Med* 2013;4:624-630.
- Eng CM, Smallwood LH, Rainiero MP, Lahey M, Ward SR, Lieber RL. Scaling of muscle architecture and fiber types in the rat hindlimb. *J Exp Biol* 2008;211:2336-2345.
- Hentzen E, Lahey M, Peters D, Mathew L, Barash I, Fridén J, *et al.* Stress-dependent and stress-independent expression of the myogenic regulatory factors and the MARP genes after eccentric contractions. *J Physiol (Lond)* 2006;570:157-167.
- Weibel ER. Practical methods for biological morphometry. In: *Stereological methods*. New York: Academic Press; 1980.
- Weibel ER. Point counting methods: practical methods for biological morphometry. London: Academic Press; 1979. 101 p.
- Talmadge RJ, Roy RR. Electrophoretic separation of rat skeletal muscle myosin heavy-chain isoforms. *J Appl Physiol* 1993;75:2337-2340.
- Lutz GJ, Cuizon DB, Ryan AF, Lieber RL. Four novel myosin heavy chain transcripts in *Rana pipiens* single muscle fibres define a molecular basis for muscle fibre types in the frog. *J Physiol (Lond)* 1998;508:667-680.
- Baldwin KM, Valdez V, Herrick RE, MacIntosh AM, Roy RR. Biochemical properties of overloaded fast-twitch skeletal muscle. *J Appl Physiol* 1982;52:467-472.
- Fortuna R, Vaz MA, Youssef AR, Longino D, Herzog W. Changes in contractile properties of muscles receiving repeat injections of botulinum toxin (Botox). *J Biomech* 2011;27:292-298.
- Kao I, Drachman DB, Price DL. Botulinum toxin: mechanism of presynaptic blockade. *Science* 1976;193:1256-1258.
- De Paiva A, Meunier F, Molgó J, Aoki K, Dolly O. Functional repair of motor endplates after botulinum neurotoxin type A poisoning: biphasic switch of synaptic activity between nerve sprouts and their parent terminals. *Proc Natl Acad Sci USA* 1999;96:3200-3205.
- Silinsky EM. On the mechanism by which adenosine receptor activation inhibits the release of acetylcholine from motor nerve endings. *J Physiol* 1984;346:243-256.
- Gillies AM, Lieber RL. Structure and function of the skeletal muscle extracellular matrix. *Muscle Nerve* 2011;44:318-331.
- Lieber RL, Ward SR. Cellular mechanisms of tissue fibrosis. 4. Structural and functional consequences of skeletal muscle fibrosis. *Am J Physiol Cell Physiol* 2013;305:C241-252.
- Labeit S, Kolmerer B. Titins: giant proteins in charge of muscle ultrastructure and elasticity. *Science (Wash)* 1995;270:293-296.
- Thacker BE, Tomiya A, Hulst JB, Suzuki KP, Bremner SN, Gastwirt RF, *et al.* Passive mechanical properties and related proteins change with botulinum neurotoxin A injection of normal skeletal muscle. *J Orthop Res* 2012;30:497-502.
- Smith LR, Pontén E, Ward SR, Chambers H, Subramaniam S, Lieber RL. Novel transcriptional profile in wrist muscles from cerebral palsy patients. *BMC Med Genomics* 2009;14:44-56.
- Smith LR, Lee KS, Ward SR, Chambers HG, Lieber RL. Hamstring contractures in children with spastic cerebral palsy result from a stiffer extracellular matrix and increased in vivo sarcomere length. *J Physiol* 2011;589:2625-2639.
- Fridén J, Lieber RL. Spastic muscle cells are shorter and stiffer than normal cells. *Muscle Nerve* 2003;27:157-164.
- Lieber RL, Runesson E, Einarsson F, Fridén J. Inferior mechanical properties of spastic muscle bundles due to hypertrophic but compromised extracellular matrix material. *Muscle Nerve* 2003;28:464-471.
- Lieber RL, Fridén J. Spasticity causes a fundamental rearrangement of muscle-joint interaction. *Muscle Nerve* 2002;25:265-270.
- Mathewson MA, Ward SR, Chambers HG, Lieber RL. High resolution muscle measurements provide insights into equinus contractures in patients with cerebral palsy. *J Orthop Res* 2015;33:33-39.
- Francisco GE. Botulinum toxin: dosing and dilution. *Am J Phys Med Rehabil* 2004;83(suppl):S30-37.